§5 Diagnostics:

Depend on what is analyzed. Typical choices:

- Moments – statistical sums over the particle distribution (slices and full beam), often plotted as time histories as the beam evolves in the accelerator:

centroid: $x_c = \langle x \rangle_\perp$ ..... etc.

RMS Widths: Beam Size $r_x = 2\langle (x-x_c)^2 \rangle^{1/2}$, ... etc.

Emittance: $\varepsilon_x = 16\left[\langle (x-x_c)^2\rangle\langle (x'-x_c')^2\rangle - \langle (x-x_c)(x'-x_c')\rangle^2\right]^{1/2}$,

etc.

Here; $\langle \cdots \rangle_\perp = \frac{1}{N_s}\sum_{i}^{\text{slice}} \{\cdots\}_i$ ..... etc.

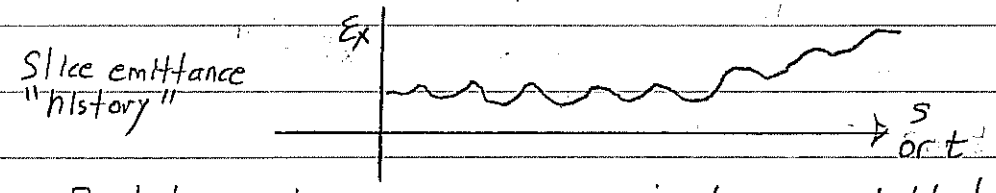

- Particle phase-space projections plotted as snapshots in time (x-x', y-y', x-y, x'-y', ...).

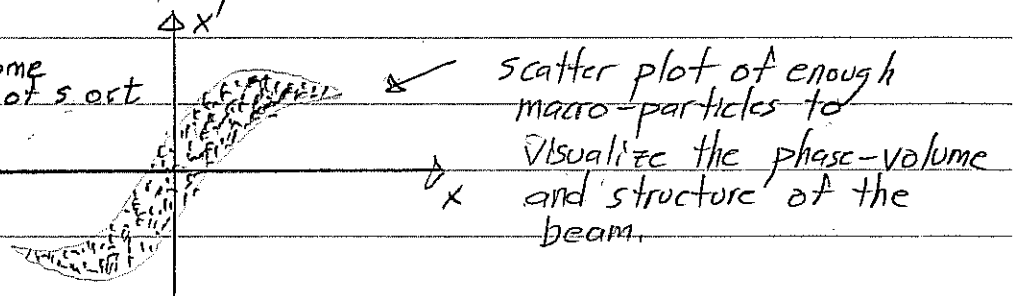

Plotting snapshots at periodic locations allows visualization of the evolution of beam distortions:

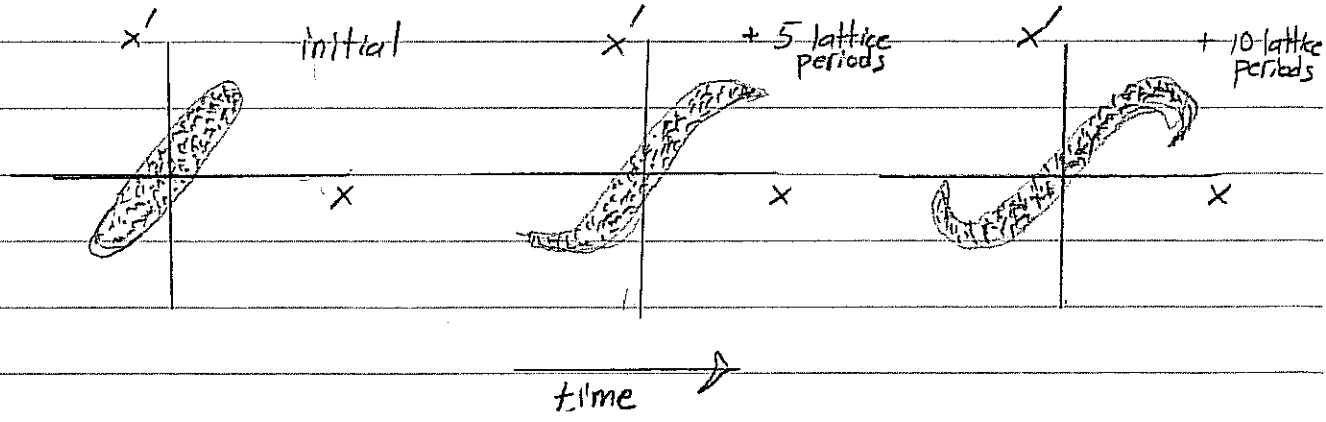

• Field Diagnostics:

Contours of self and applied fields illustrate field structure.

Examples:

1) Total potential contors of ϕ (self and applied) of an elliptical beam in an electric quadrupole formed by 4 biased rods.

same ϕ contours with beam particles plotted

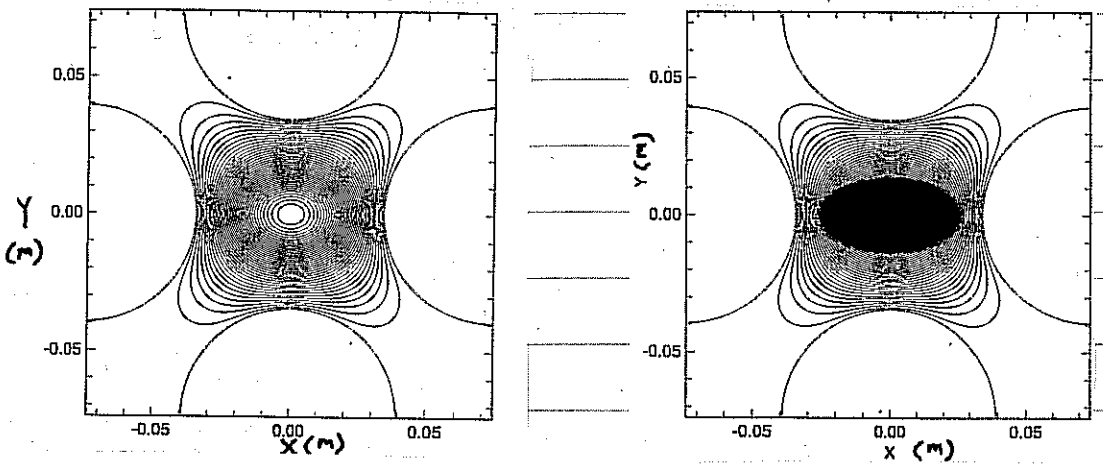

2) Applied Field Scalar magnetic potential contours of a permanant magnet lense illustrate the structure of applied field nonlinearities:

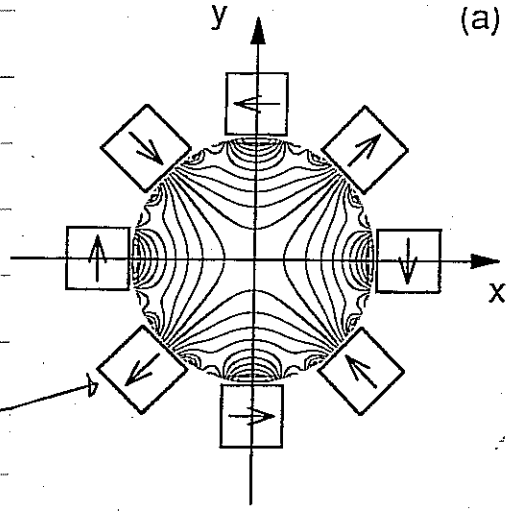

8 Block Permanent Magnet Quadrupole.

Permanent Magnet

Note: contours deviate from hyperbolic near aperture edge.

Numerous other field diagnostics are possible:

- Field energy, multipole moments,

§6 Particle Loads

To start the simulation, one must specify and "load" the initial distribution function.

In realistic accelerators, focusing elements are s-varying. In such situations there are in general no known equilibrium distribution functions. Moreover, it is unclear in most cases if the beam is even best thought of as an equilibrium + perturbations as is typical in plasma physics. Rather, in accelerators, the beam is injected from a source and may only reside in the machine (especially a linac) for a small number of characteristic oscillation periods and may not fully relax to an equilibrium-like state. In such situations, so-called "source-to-target" simulations where the particles are simulated off the source and tracked to the target can be most realistic if carried out with realistic focusing fields, accelerating waveforms, alignment errors, etc.

Unfortunately, such idealized source-to-target simulations can rarely be carried out due to computer limitations.

- Memory limits
- Numerical convergance and accuracy ...

Two ways around this limitation:

1) Load experimentally measured distribution at some point in the machine and advance as an initial condition.
2) Load an idealized initial distribution.

The 1st option can have practical difficulties:

- Diagnostics often are far from an ideal 6D "snapshot" of the beam phase-space.
  - Much information typically lost.
- Process of measuring the beam can itself change the beam.

Most commonly, some experimental measures such as:

- rms beam sizes r_x, r_y, r_x', r_y'
- rms emittances $\varepsilon_x, \varepsilon_y$

are loaded in the form of idealized distributions.

It can be insightful to initialize the beam in a simplified manner

- Fewer simultaneous processes can allow one to more clearly see how limits arise.
- Seed perturbations of relevance when analyzing resonance effects, instabilities, halo, etc.

In these situations it is often useful to load a round, continuously focused distribution such as:

- Thermal Equilibrium
- Waterbag
- KV

and then transform the particle coordinates to "match" the local focusing structure of the lattice using a local KV envelope solution:

$$\frac{d^2}{ds^2} r_x(s) + \kappa_x(s) r_x(s) - \frac{2Q(s)}{r_x(s)+r_y(s)} - \frac{\varepsilon_x^2(s)}{r_x^3(s)} = 0$$

$$\frac{d^2}{ds^2} r_y(s) + \kappa_y(s) r_y(s) - \frac{2Q(s)}{r_x(s)+r_y(s)} - \frac{\varepsilon_y^2(s)}{r_y^3(s)} = 0$$

$\kappa_x(s)$, $\kappa_y(s)$ = lattice focusing constants

$Q(s)$ = local perveance (specified)

$\varepsilon_x(s)$, $\varepsilon_y(s)$ = local emittances (specified)

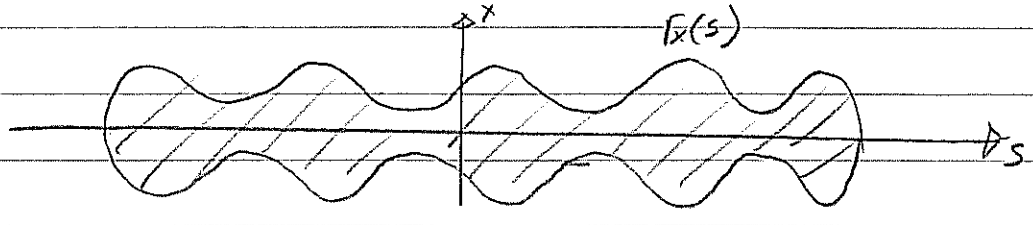

Procedure:

1st

Load in each $\perp$ slice round, continuous distribution:

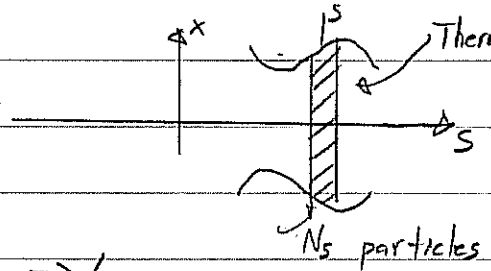

$$r_b = \sqrt{r_x r_y}$$

$$\varepsilon_b = \sqrt{\varepsilon_x \varepsilon_y}$$

$\Rightarrow$ $\vec{X}_i$, $\vec{X}_i'$ specified

2nd

Transform the spatial coordinates to match the elliptical envelope structure

$$x_i \longrightarrow \frac{r_x}{r_b} x_i$$

$$y_i \longrightarrow \frac{r_y}{r_b} y_i$$

3rd

Transform the local thermal velocity spreads to obtain the right average thermal force.

$$x_i' \longrightarrow \frac{\varepsilon_x}{\varepsilon_b} \frac{r_b}{r_x} x_i'$$

$$y_i' \longrightarrow \frac{\varepsilon_y}{\varepsilon_b} \frac{r_b}{r_y} y_i'$$

4th

Add the correct coherent velocity to match the needed envelope angle.

$$x_i' \longrightarrow x_i' + r_x' \frac{x_i}{r_x}$$

$$y_i' \longrightarrow y_i' + r_y' \frac{y_i}{r_y}$$

// Aside – The semi-Gaussian Distribution

It is not necessary to always load something based on a transformation of an equilibrium distribution to get a good quiescent load. Note that for high space-charge intensities:

- Beam space charge will be more or less uniform out to the edge, where the density will rapidly fall to zero.

- If the beam is injected off a uniform temperature source or has relaxed, one expects roughly uniform thermal velocity spread across the cross-section of the beam.

This suggests the so-called "semi-Gaussian" load specified as follows:

- Uniform density within an elliptical beam envelope.

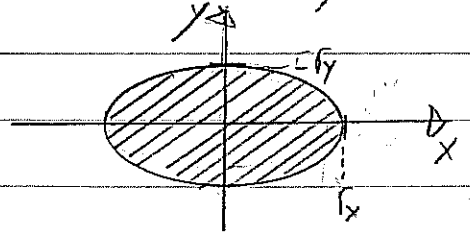

x_i, y_i uniformly distributed for $(x/r_x)^2 + (y/r_y)^2 \le 1$.

- Gaussian distributed thermal velocity spread with the correct coherent velocity to match the needed envelope angles

$$x_p' = r_x' \frac{x_i}{r_x} + \frac{\varepsilon_x}{2r_x} \tilde{r}_{x_i}$$

$$y_i' = r_y' \frac{y_i}{r_y} + \frac{\varepsilon_y}{2r_y} \tilde{r}_{y_i}$$

$\tilde{r}_{x,y_i}$ Gaussian distributed with unit variance $\left(\frac{1}{N_s}\sum_{i}^{slice} \tilde{r}_{x,y_i}^2 = 1\right)$

The semi-Gaussian load results in "squared" initial x-x' and y-y' phase space projections!

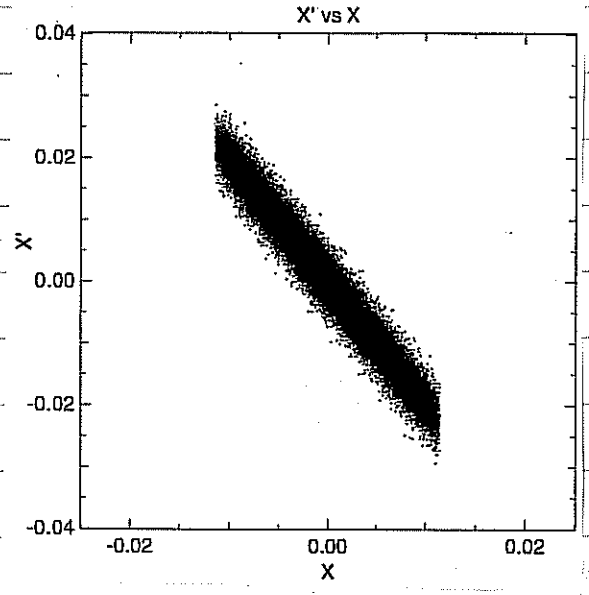

Initial load in a symmetric FODO AG Quadrupole transport lattice

The unphysical edges typically relax rapidly without perturbing the low order RMS structure of the beam (envelope match, emittance, etc.).

1 lattice period advance

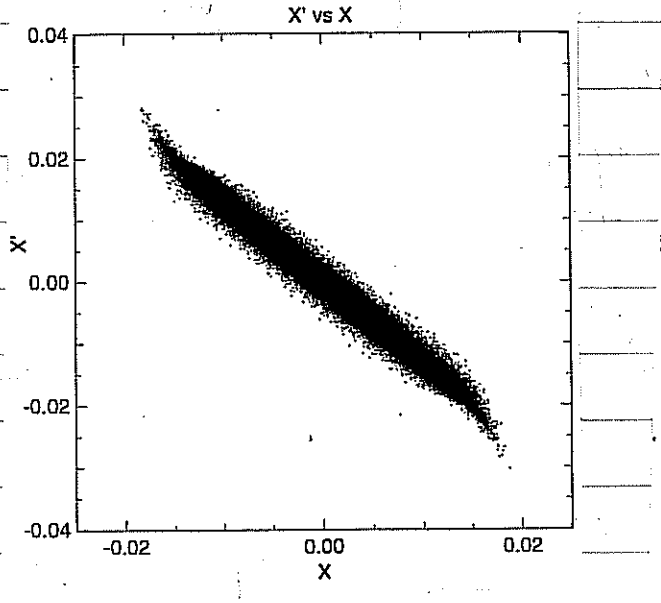

4 lattice period advance

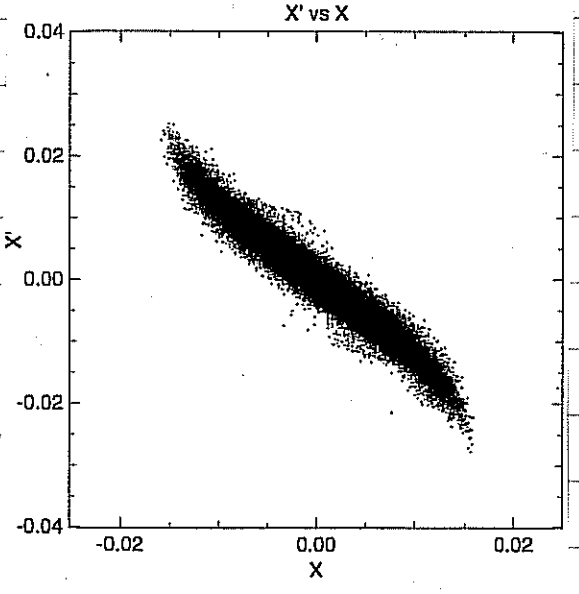

Numerous other loading techniques exist to address specific issues.

//

§7 Numerical Convergence

Numerical simulations must be checked for proper resolution and statistics to be confident that answers obtained are correct and physical.

Resolution on discretized quantities
- Time step in particle advance
- Spatial grid for fields

Statistics (number of macroparticles) to control noise.

More resolution and statistics require more computer time and memory. To be practical, one generally wishes to solve problems with the minimum resources required to achieve correct, converged answers. Unfortunately, there are no set rules on what resolution and statistics are required. This depends on what one is examining, how long the simulations are run, what numerical methods are employed, ...

Some general guidance:

- The statistical rms emittances:

$$\varepsilon_x = 4\left[\langle x^2\rangle_\perp\langle x'^2\rangle_\perp - \langle xx'\rangle_\perp^2\right]^{1/2}$$

$$\varepsilon_y = 4\left[\langle y^2\rangle_\perp\langle y'^2\rangle_\perp - \langle yy'\rangle_\perp^2\right]^{1/2}$$

and easy to interpret
often prove to be sensitive measures of numerical differences when plotted as overlaid time histories.
  - picks up small phase space distortions induced by numerical errors.

general guidance continued ....

- To get started, find results from similar problems using similar methods.

- Benchmark code and methods against problems with known analytical solutions, established codes using both similar and different numerical methods, ...

- Recheck numerical convergence whenever runs differ significantly or when differing quantities are analyzed.

  - What is adequate for one measure of the beam (say image charge structure) may not be for another (say collective modes).

- Although it is common to increase resolution and statistics till relevant quantities do not vary, it is also useful to purposefully analyze poor resolution and statistics regimes so the characteristics of unphysical numerical errors can be recognized.

- Expect to make many setup, convergence, and debugging runs for each useful series of simulations carried out.

Specific Numerical Convergence Comments:

Time Resolution.

These comments are applicable to both spatial or time steps of the particle advance. We will frame estimates in terms of timesteps.

- Particle coordinates should not move through more than one cell in a single step. This is a standard "Courant" condition:

$$v_x \Delta t < \Delta x$$
$$v_y \Delta t < \Delta y$$
$$v_z \Delta t < \Delta z$$

for all particles.

- Enough steps should be taken to resolve variations in applied field structures.

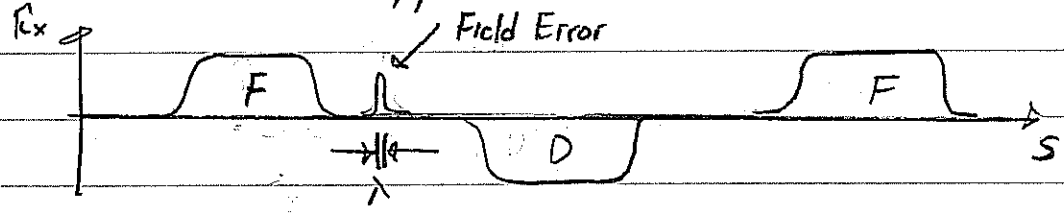

$v_s \Delta t < \lambda$; λ = shortest wavelength of field structures to be modeled

- Phase variations in collective waves (if of interest) should be resolved. For a leap-frog mover this requires:

ω = mode frequency component

$$\frac{\omega \Delta t}{2\pi} < \frac{1}{2}$$

Spatial Resolution

For cold beams the beam edge can be sharp for most reasonable distribution functions:

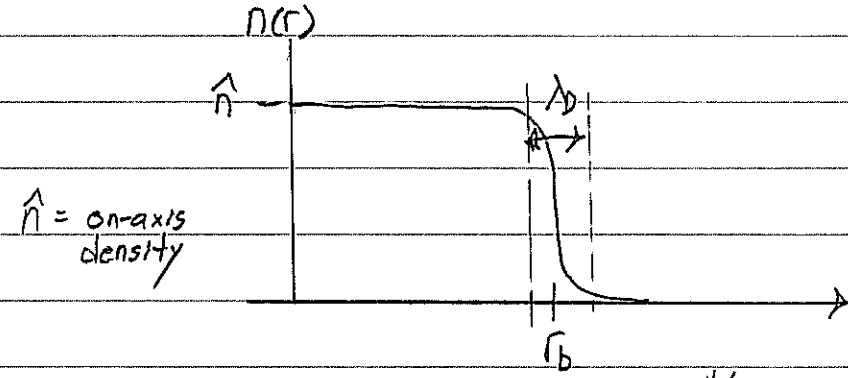

Density falls off in $\sim(\lambda_D)$

Debye length: $\lambda_D = \frac{v_t}{\omega_p} = \left(\frac{\varepsilon_0 k_B T}{\hat{n} q^2}\right)^{1/2}$

$v_t = (k_B T/m)^{1/2}$

$\omega_p = \left(\frac{q\hat{n}}{\varepsilon_0 m}\right)^{1/2}$

$r_b = \sim 5\lambda_D \rightarrow 30\lambda_D$ typical.

To resolve edge physics, the mesh should have several cells across the rapid density variation near the edge of the beam.

$$dx, dy < \frac{\lambda_{Dx,y}}{2}$$

$$\lambda_{Dx,y} = \left(\frac{k_B T_{x,y}}{m}\right)^{1/2}$$

$T_{x,y}$ = local kinetic temperature

The mesh should also resolve relevant spatial scales associated with processes of interest:

- If applied electrostatic fields are calculated from biased conductors, the mesh should resolve conductor structures or special corrections should be made.
- Self-field fluctuations induced by collective modes should be resolved.

Collective mode resolution: From Eigenfunctions to be presented later in the class:

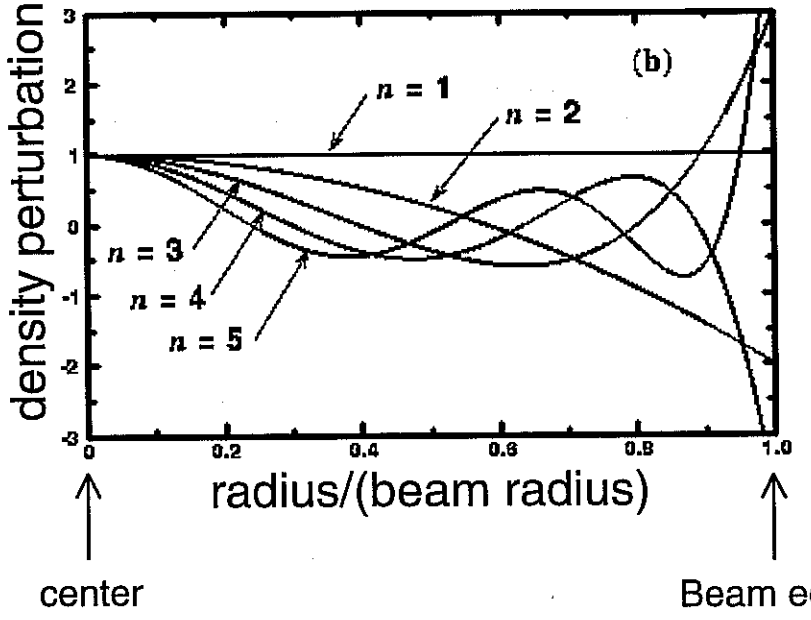

Collective mode density perturbations on a uniform density beam.

$\Rightarrow$ $dx, dy < \lambda \sim$ shortest characteristic wavelength of modes of interest.

Note that higher order modes (n larger) will become hard to resolve. Moreover, such perturbations also oscillate rapidly making time (s) stepsize resolution likewise difficult.

Statistics:

Collective effects typically require having a significant number of particles N_D within the characteristic screening radius characterized by the Debye length:

2D: $$N_D = \sum_i \int_{\substack{\text{circle} \\ |\vec{x}|<\lambda_D}} d^2x\, \delta^{(2)}(\vec{x}-\vec{x}_i) \gg 1$$

$\vec{x}_i$ = macro-particle coordinate.

3D: $$N_D = \sum_i \int_{\substack{\text{sphere} \\ |\vec{x}|<\lambda_D}} d^3x\, \delta^{(3)}(\vec{x}-\vec{x}_i) \gg 1$$

where:

$$v_t = (k_B T/m)^{1/2}$$

$$\lambda_D = \frac{v_t}{\omega_p} = \left(\frac{\varepsilon_0 k_B T}{\hat{n} q^2}\right)^{1/2} \qquad \omega_p = \left(\frac{q^2 \hat{n}}{\varepsilon_0 m}\right)^{1/2}$$

$\sum_i \Rightarrow$ sum over all macro particles.

In simulations of higher order collective modes it may also be necessary to have a significant number of particles per cell on a mesh that resolves the relevant spatial variations of mode induced self-field fluctuations.

2D: $$N_{cell} = \sum_i \int_{cell} d^2x\, \delta^{(2)}(\vec{x}-\vec{x}_i) \gg 1$$

3D: $$N_{cell} = \sum_i \int_{cell} d^3x\, \delta^{(3)}(\vec{x}-\vec{x}_i) \gg 1$$

- Larger N_{cell} prevents local self-fields from being noise dominated.
- Larger N_{cell} leads to larger N_D, typically $N_D > N_{cell}$ since λ_D must be resolved on the grid.

Good statistics are only needed in the beam core with the possible exception of certain beam-halo problems and near the beam edge.

- Most beams will only occupy a fraction of the full grid.

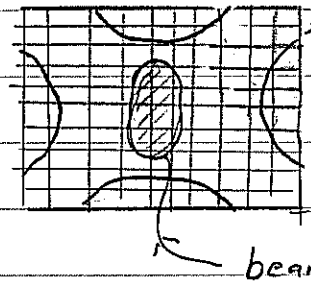

statistics should be evaluated in the cells that the beam occupies rather than average grid measures.

No comprehensive rules exist for how good the statistics must be. Individual problems must be checked and verified. Some general comments:

- What is adequate will typically depend on what is analyzed
  - Image fields may be resolved with few particles
  - Collective waves may take many particles if low noise (interpetable) diagnostic projections are needed.
- Longer runs generally require increased statistics
- Poor statistics result in unphysical collisionality that is often characterized by a linear rise in beam emittances with simulation time.

Classes of Particle Simulations.

How important is smoothing?

3D Beam: $N \sim 10^{10} - 10^{14}$ particles typical

Simulations: $N \lesssim 10^{8}$ practical (modern parallel computers), typical $10^{3} - 10^{6}$

Each simulation particle may represent: $10^{3} \rightarrow 10^{11}$ particles in the real beam for 3D simulations.

- Smoothing involved with particle weightings are key to obtaining physical answers and limiting collisionality.

Is the situation really this bad?

- Lower dimensonal models typically simulated.

3D Model

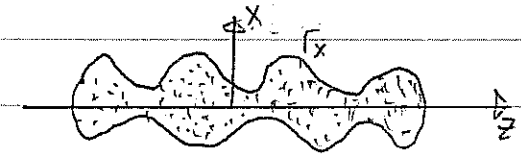

N point particles with smoothed interactions

Phase Space: x, y, z ; p_x, p_y, p_z } 6D

Physical charge – point charges

$$\rho = \sum_i q\, \delta(x-x_i)\,\delta(y-y_i)\,\delta(z-z_i)$$

Smoothed charge

$$\rho = \sum_i q_M\, f(x-x_i, y-y_i, z-z_i)$$

q_M: Macro particle charge

f: smoothed shape function

2D – Thin Slice Model

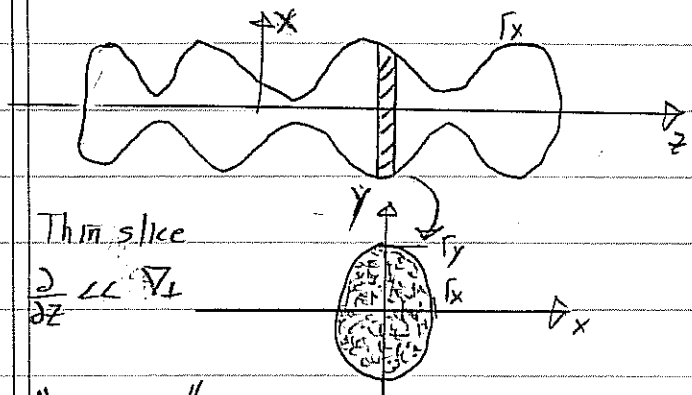

N line charges with smoothed interactions.

Thin slice

$\frac{\partial}{\partial z} \ll \nabla_\perp$

Phase Space:

x, y } 4D + possible 1D
p_x, p_y }

p_z

4D or 5D

"Physical" charge – line charges

$$\rho = \sum_i \lambda_p \delta(x-x_i)\delta(y-y_i)$$

Smoothed charge –

λ_M = Macro particle line charge

f = smoothing function

$$\rho = \sum_i \lambda_M f(x-x_i, y-y_i)$$

The slice must be tracked in s with each particle moving the same increment in s with each step so that a slice maps to a slice.

- If p_z is included the velocity distribution must be assumed "frozen in".

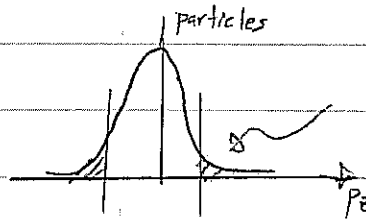

parts that would leave assumed replenished by particles from adjacent slices.

- Response to acceleration may be modeled with

- "Thick" slice models also possible with periodic boundary conditions, on the "slice" to try to recover some 3D effects of a long pulse in a periodic lattice.

2D r-z Model

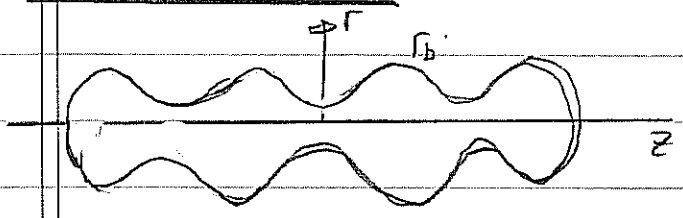

N charged Rings with smoothed interactions

$\partial/\partial\theta = 0$ Axisymmetric

Phase Space.

r, z } 4D + possible 1D
p_r, p_z }

p_θ (angular mom.)

4D or 5D.

physical charge - cylindrical rings

$$\rho = \sum_i \frac{Q_i}{2\pi} \frac{\delta(r-r_i)\delta(z-z_i)}{r_i}$$

smoothed charge

$$\rho = \sum_i \frac{Q_M}{2\pi} \frac{f(r-r_i, z-z_i)}{r_i}$$

Q_M : Macro particle charge
f : Smoothing function.

- Used to model solenoidal transport of an initial axisymmetric beam.
- Sometimes used to model AG beams with an approximately equivalent, s-dependant focusing force. $\vec{x}_\perp'' = k_{p0}^2(s)\vec{x}_\perp + \cdots\cdots$

1D Axisymmetric Model

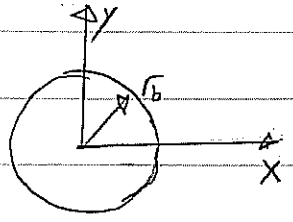

N charged cylinders with smoothed interactions

$\partial/\partial\theta = 0$

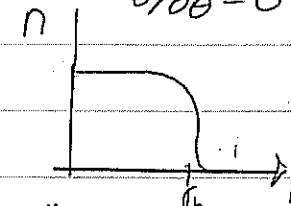

Phase - Space

r } 2D + possible
p_r }

p_θ, p_z

2D to 4D

"physical" charge - cylindrical sheets

$$\rho = \sum_i \frac{Q_i}{2\pi} \frac{\delta(r-r_i)}{r_i}$$

smoothed charge

$$\rho = \sum_i \frac{Q_M}{2\pi} \frac{f(r-r_i)}{r_i}$$

Q_M : Macro charge
f : Smoothing function

- Simple model for continuously focused, axisymmetric beams

1D slab Model

N charged slabs with smoothed interactions.

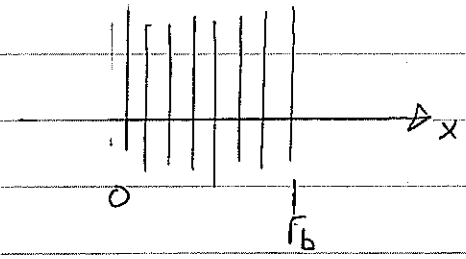

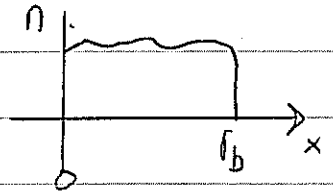

Phase-Space

x, p_x } 2D + possible p_y, p_z

2D to 4D

"physical" charge - sheets

$$\rho = \sum_i \sigma\, \delta(x - x_i)$$

smoothed charge

$$\rho = \sum_i \sigma_M\, f(x - x_i)$$

σ_M: macro particle charge

f: smoothing function

- Most simple model, but slab geometry is least physical.

It is not immediately clear how such different models can in many cases represent qualitatively similar collective interactions since force laws can change form with dimension. For example, in free space, we find that:

Model	Free space. Field due to ith "particle"	
3D	$\vec{E} = \frac{q_i (\vec{x} - \vec{x}_i)}{4\pi\varepsilon_0 \lvert\vec{x} - \vec{x}_i\rvert^3}$	
2D	$\vec{E} = \frac{\lambda_i (\vec{x} - \vec{x}_i)}{2\pi\varepsilon_0 \lvert\vec{x} - \vec{x}_i\rvert^2}$	λ_i = line-charge "particle"
1D	$E_x = \frac{\sigma_i (x - x_i)}{2\varepsilon_0 \lvert x - x_i\rvert}$	σ_i = sheet charge "particle"

The reason these radically different interactions can give similar physics is that the screening associated with collective interactions is found to be similar:

- Debye screening has similar characteristics in each dimension.

Showed 2D form, in class. Will show in final that the 3D scaling obtains the same Debye length definition. $\Rightarrow$

$$\lambda_D = \frac{v_{thermal}}{\omega_p} = \left(\frac{\epsilon_0 k_B T}{\hat{n} q^2}\right)^{1/2} \qquad v_t = (k_B T/m)^{1/2}$$

$$\omega_p = \left(\frac{q^2 \hat{n}}{\epsilon_0 m}\right)^{1/2}$$

- It is much easier to have a significant number of particles within the characteristic screening distances for lower dimensional problems.

  - Lower dimensional simulations can more easily resolve collective effects!
    (Sometimes people run 3D simulations for collective modes and present garbage answers due to resolution difficulties)

// Example

$q = Ze$ ions, $e = 1.6 \times 10^{-19}$ C

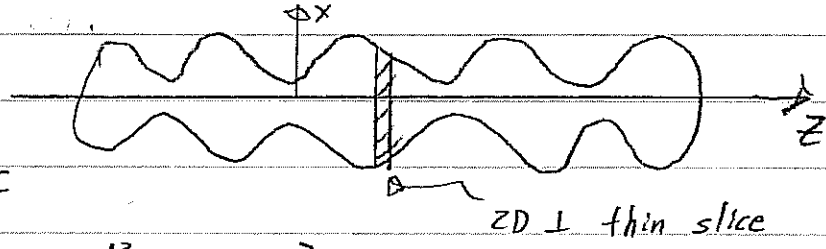

$\lambda \sim 10^{-13} \rightarrow 10^{-7}$ C/m typical for intense beams

$$\frac{\#\ particles}{cm} = \frac{\lambda}{Ze \cdot 100} \sim \frac{10^4}{Z} \rightarrow \frac{10^{10}}{Z}$$

$q = Ze$ (Z: charge state)

- Smoothing still important in lower dimensions and real beam is 3D

//

S.M. Lund Clay

WARP Code Overview

Electrostatic Multi-dimensional PIC Code

WARP3d – x, y, z, p_x, p_y, p_z
Moves int
Many Fieldsolvers!
SOR, Multigrid, FFT,
FFT + Tridiag, FFT + Cap Ma

WARPxy – x, y, p_x, p_y, p_z
Moves in s

WARPrz – r, z, p_r, p_z p_θ
Moves in t

WARPenv – envelope solver
used to seed / load PIC
r_x, r_y, r_x', r_y'
Advances in s

Hermes – Fluid II + Bridded
Space Charge Field

- Common diagnostic tools built around gist. graphics
- Run with python interpreter

Example Script
"ag-slice.py"

3D PIC simulations are being used to guide retrofits of an existing ESQ injector at LBL

1st principles, mid-pulse 3D simulations have been carried out to guide injector retrofits aimed at decreasing beam aberrations

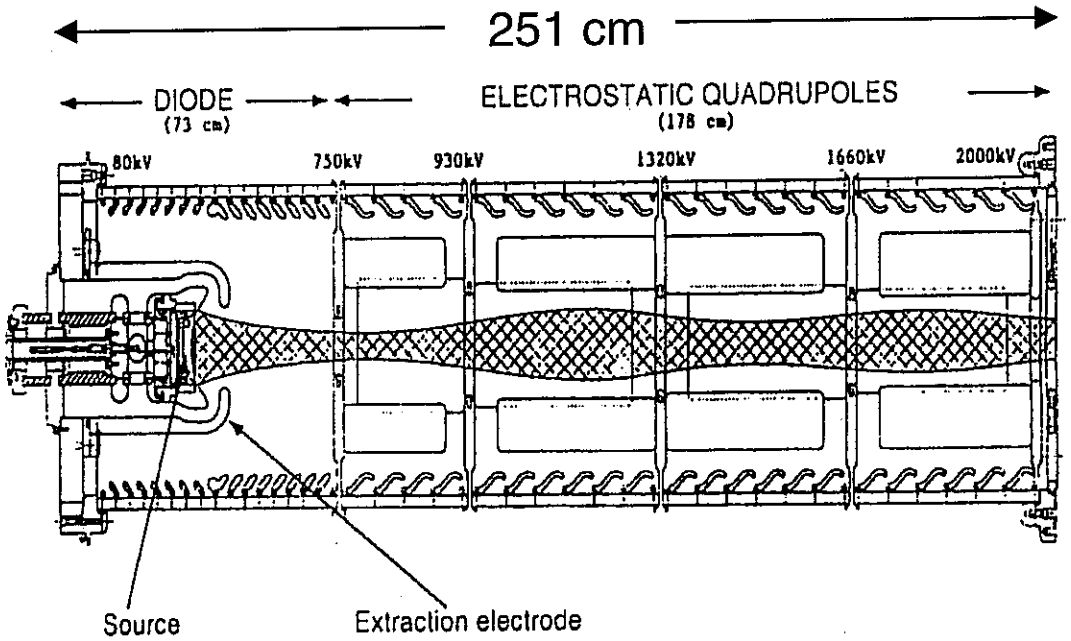

Multi-Shot Film Images of Beam at Injector Exit

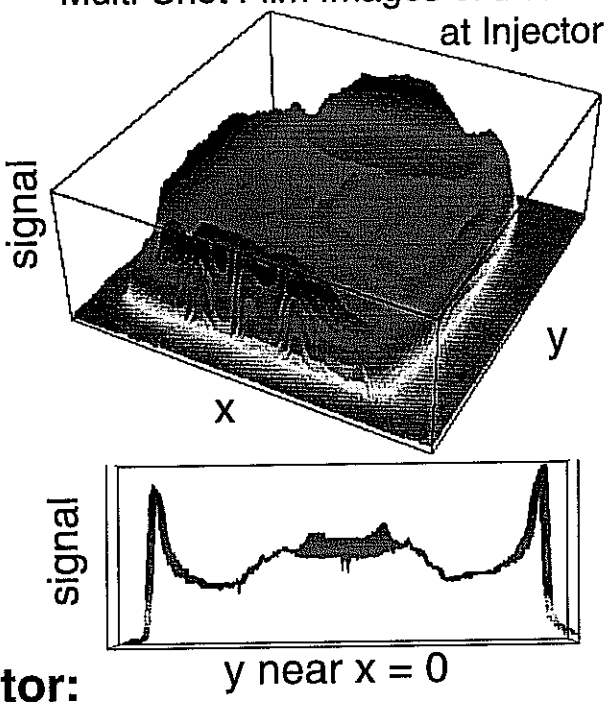

Parameters expected at exit of retrofitted injector:

Energy:	**E = 1.71 MeV**	
Current:	**I = 692 mA, K**	
Emittance:	**ε_n = 1.1 π mm-mrad**	**rms edge measure**
	~ 0.7 π mm-mrad	**measure eliminating empty entrained space**
Envelope:	**r_x = 56.3 mm**	**r_x' = 53.8 mrad**
	r_y = 55.7 mm	**r_y' = -44.8 mrad**

8/10 Example PIC Simulations SM Lund 54/

HCX Injector: Simulations show distribution distortions in the retrofitted injector should be more modest

Mid-pulse distribution projections at exit plane of injector

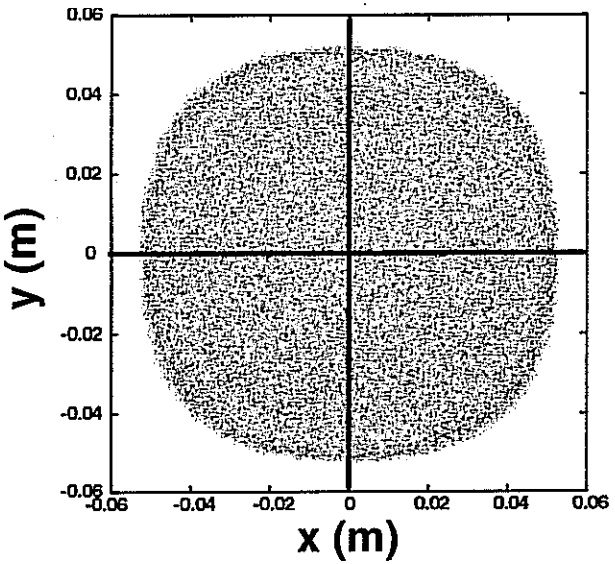

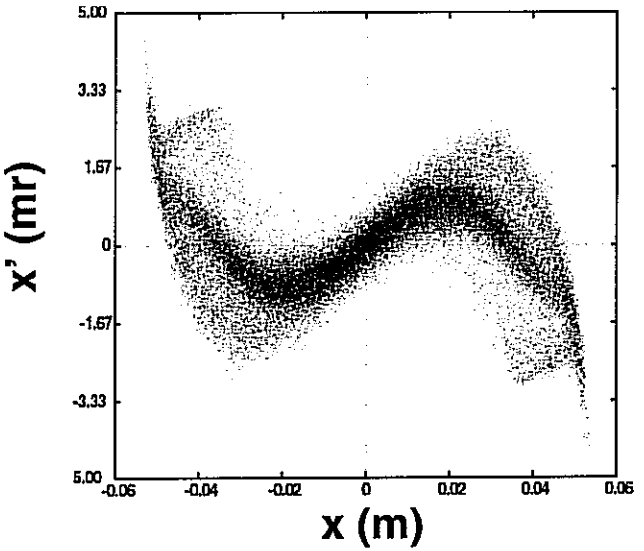

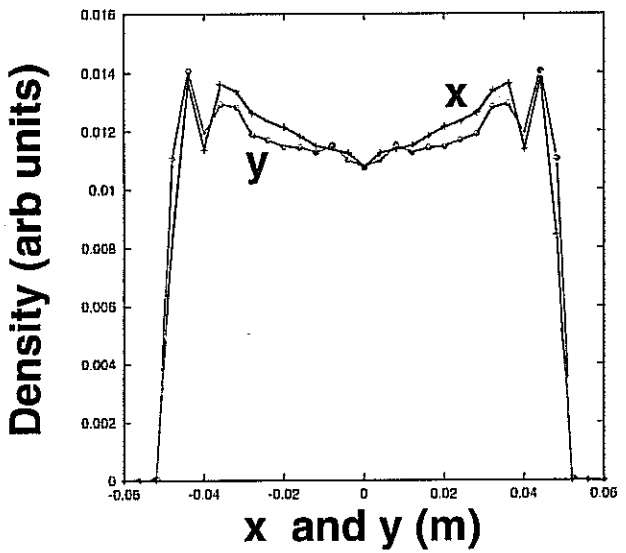

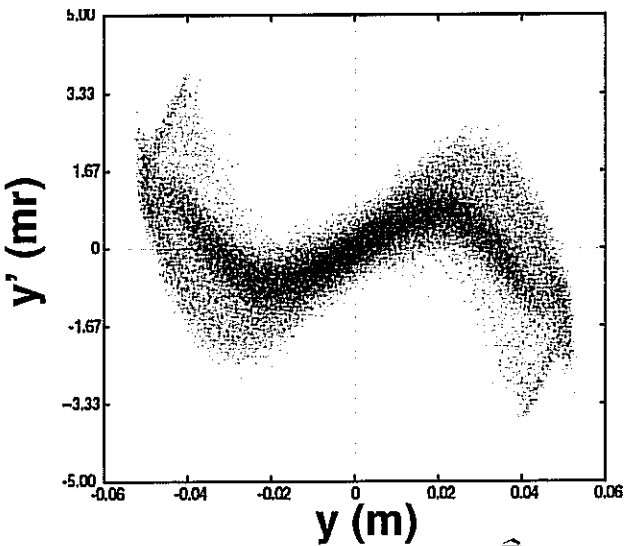

Overall convergence and divergence angles removed to illustrate distortions

SM1 Lund 55/

Simulations show how waveform rise-time determines beam head mismatch

Tuned 1d diode voltage waveform rise-time is 400 ns -- deviations from this lead to significant mismatch effects in the beam head and particle loss with resultant worries about breakdown, electron effects, etc.

Rise-time τ = 800 ns

beam head particle loss < 0.1%

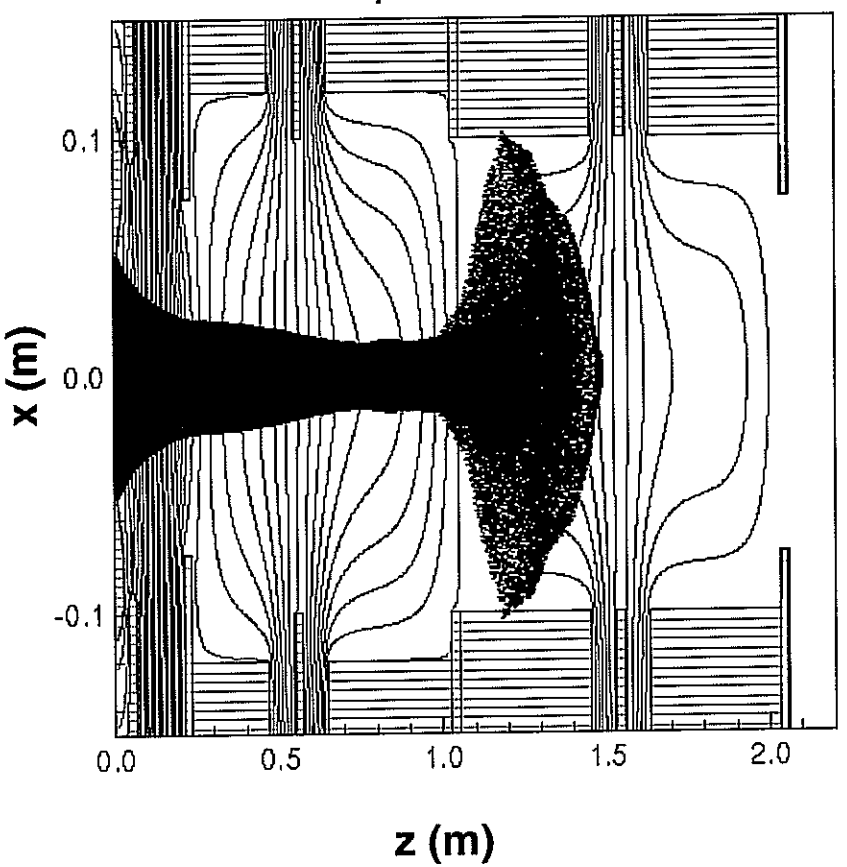

Rise-time τ = 400 ns

zero beam head particle loss

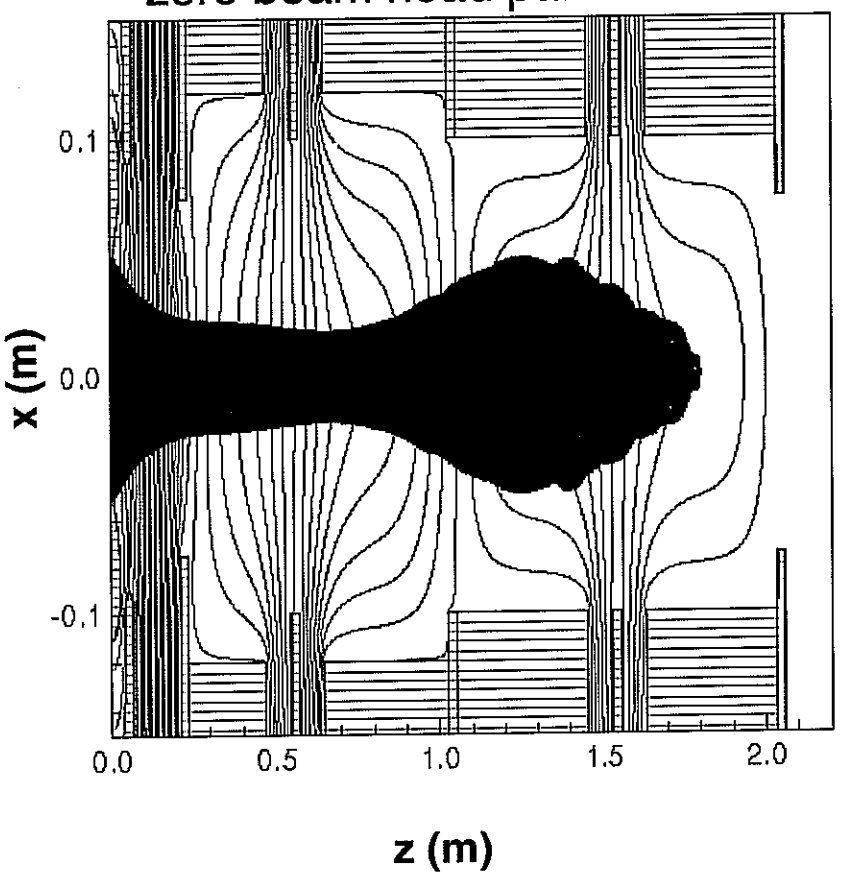

S.M. Lund 5/...

Initial distribution distortions will launch a spectrum of collective mode perturbations that evolve

Kinetic and fluid theories have been employed to analyze perturbations on a uniform density intense-beam equilibrium [Lund and Davidson, Phys. Plasmas, 5 3028 (1998)]

Small Amplitude Perturbations (arbitrary units, kinetic and fluid theory)

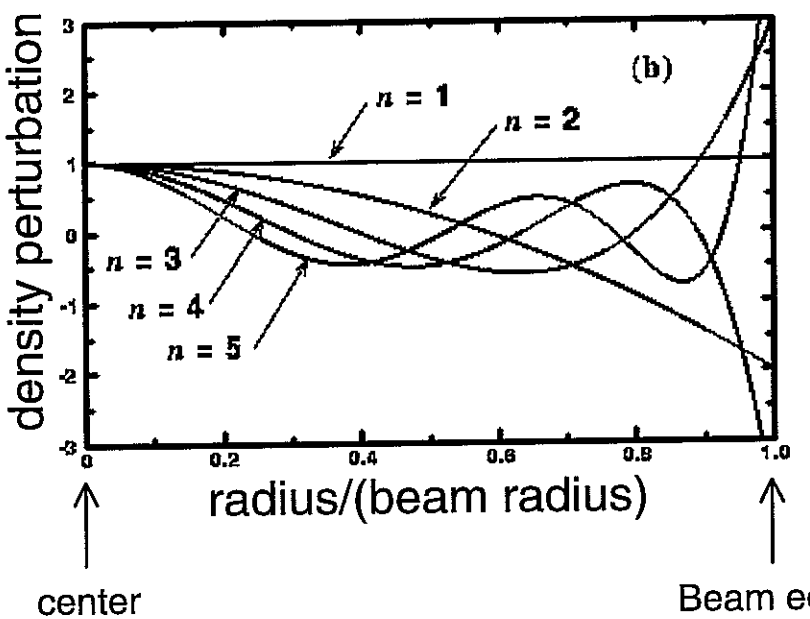

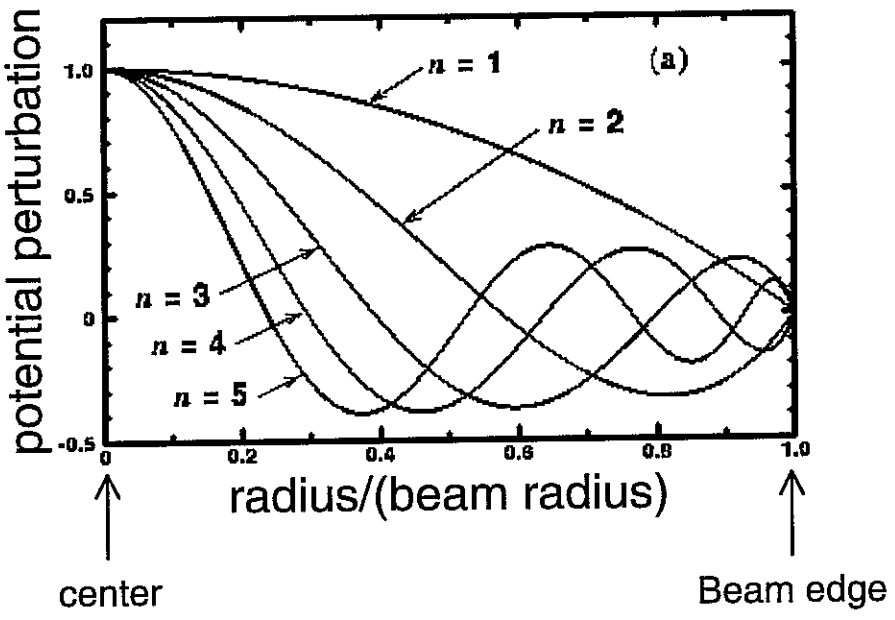

Mode Dispersion Relation (fast branch, from fluid theory)

$$\frac{\sigma_n}{\sigma_0} = \sqrt{2 + 2\left(\sigma/\sigma_0\right)^2 (2n^2 - 1)}$$

σ_n = mode phase advance

n = 1,2,3, ...

Example:

$\sigma_0 = 80^o$, $\sigma/\sigma_0 = 0.2$

$\sigma_1 = 115^o$, $\sigma_5 = 182^o$, ...

SM, Lund 57

Perturbations launched by initial distribution nonuniformities can phase-mix to a more uniform profile with increased emittance

Mode spectrum launched can undergo a rapid cascade, settling to a smaller amplitude and lower order distortion

- Approximate conservation constraints employed to bound emittance increases resulting from full relaxation to a uniform profile [Lund, Lee, and Barnard, Proc. Linac 2000, pg. 290]
- How will such evolutions influence the range and interpretation of measurements

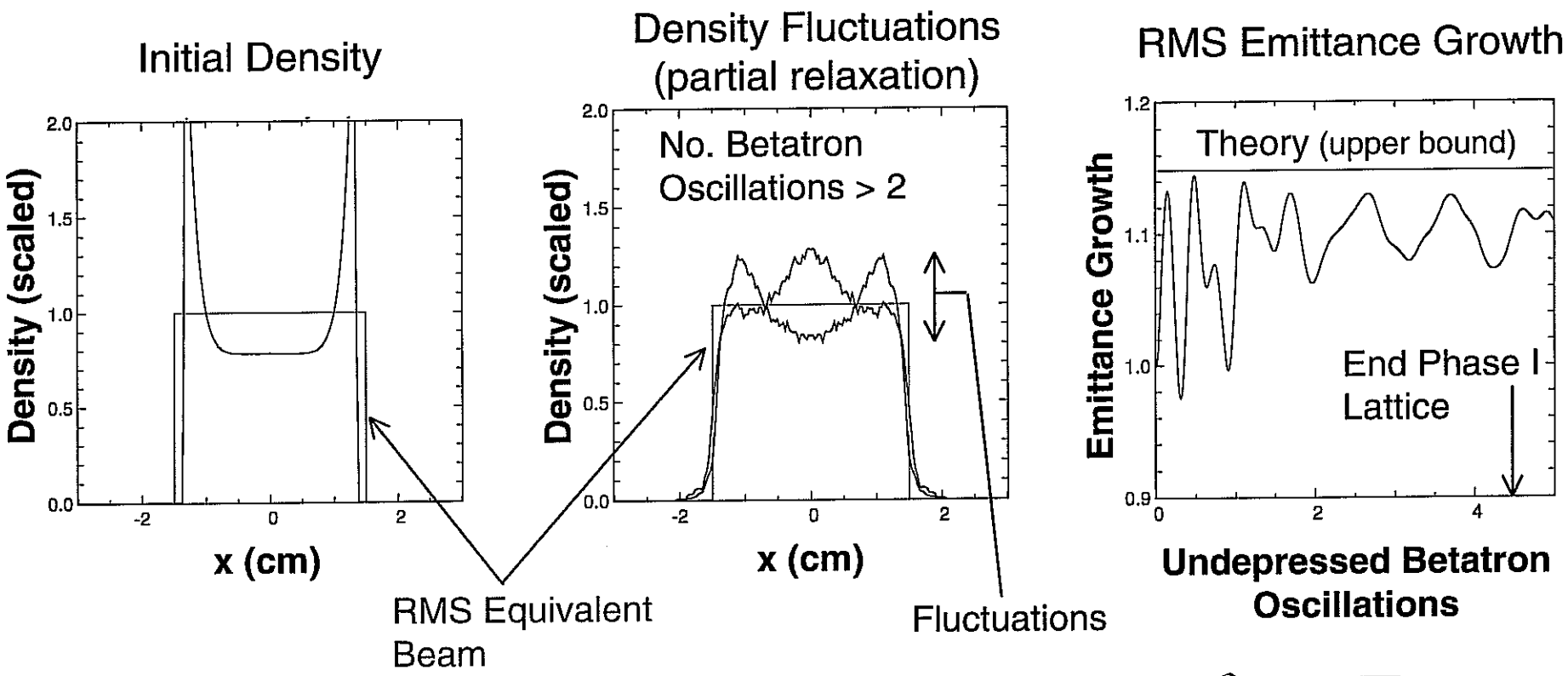

SM, Lund '85

Analytic theory has been used to parametrically bound emittance growth due to the relaxation of space-charge nonunifomities

Approximate conservation constraints can be employed to estimate maximal emittance increases resulting from the relaxation of an initial nonuniform density profile to a final, uniform profile [Lund, Lee, and Barnard, Proceedings Linac 2000, Monterey, CA, pg. 290]

Initial Density

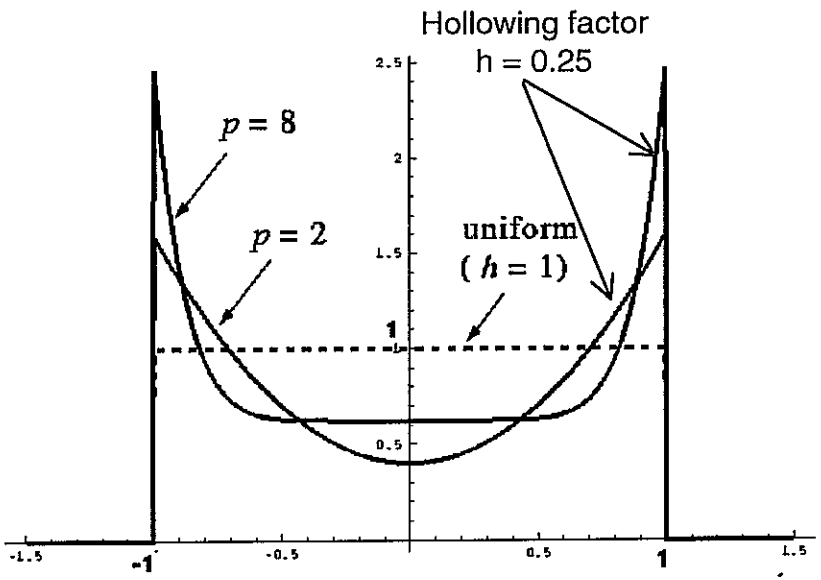

Normalized Radial Coordinate

hollowing ~ r^p

h = ratio min to max density

Emittance Growth on Relaxation

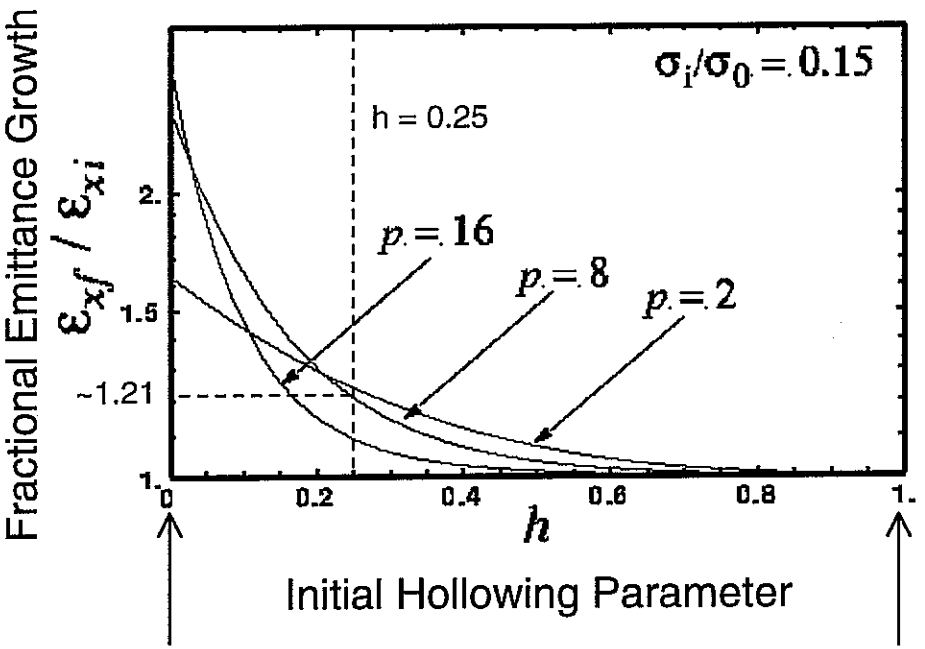

Initial Hollowing Parameter

Extremely Hollowed

Uniform

S.M. Lund, 5/

HCX Phase II: A wide range of parametric simulations have been carried out with realistic magnetic transport lattices

A syncopated magnetic transport lattice of ~ 50 lattice periods has been designed

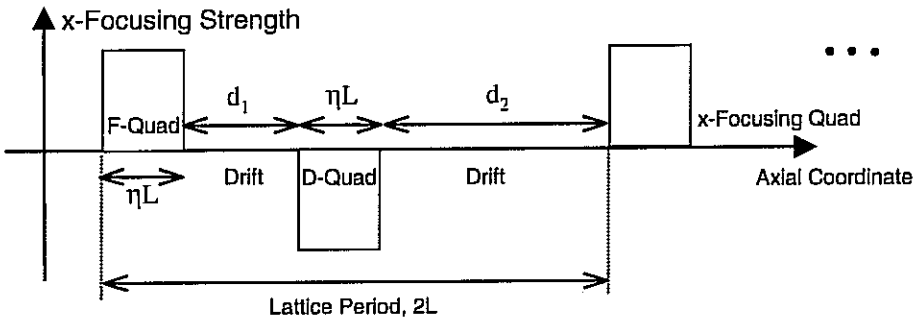

η = Quadrupole Occupancy $(0 < \eta < 1)$ HCX: $\eta = 0.453$

α = Syncopation Factor $(0 < \alpha < 1)$ $\alpha = 0.248$

Drifts:

$d_1 = \alpha(1-\eta)\eta L$

$d_2 = (1-\alpha)(1-\eta)\eta L$

Superconducting magnetic quadrupoles have been designed and prototyped

$r_p = 29.5$ mm $\quad B_q' = 104$ T/m (max) $\quad B_q \sim 6$ Tesla (wire)

$\ell = 136$ mm $\quad \ell_{eff} = 101$ mm $\quad$ Integrated Field Error $< 15 \times 10^{-3}$

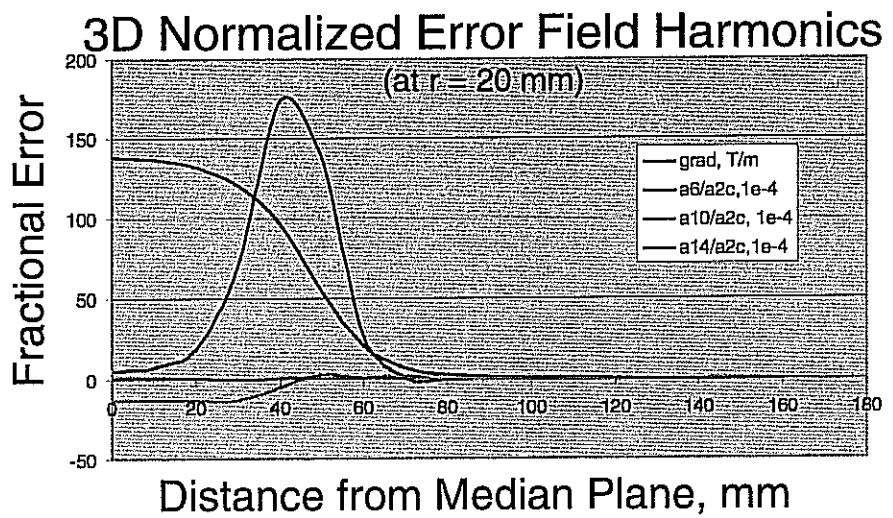

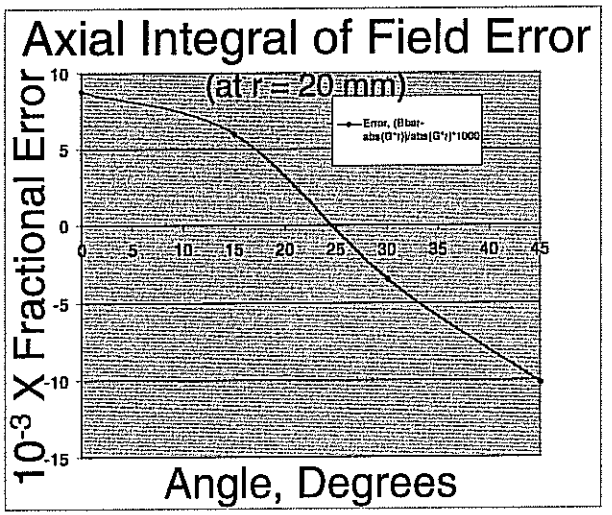

The Heavy Ion Fusion Virtual National Laboratory

PPPL PRINCETON PLASMA PHYSICS LABORATORY

S.M. Lund 10/09

HCX Phase II: Processes influencing beam quality and control have been explored --- Example: Nonlinear applied fields and beam quality

Full 3D magnetic field is resolved as:

$$\vec{B} = \vec{B}_{quad} + \delta\vec{B} \qquad \delta\vec{B} \rightarrow s \cdot \delta\vec{B}$$

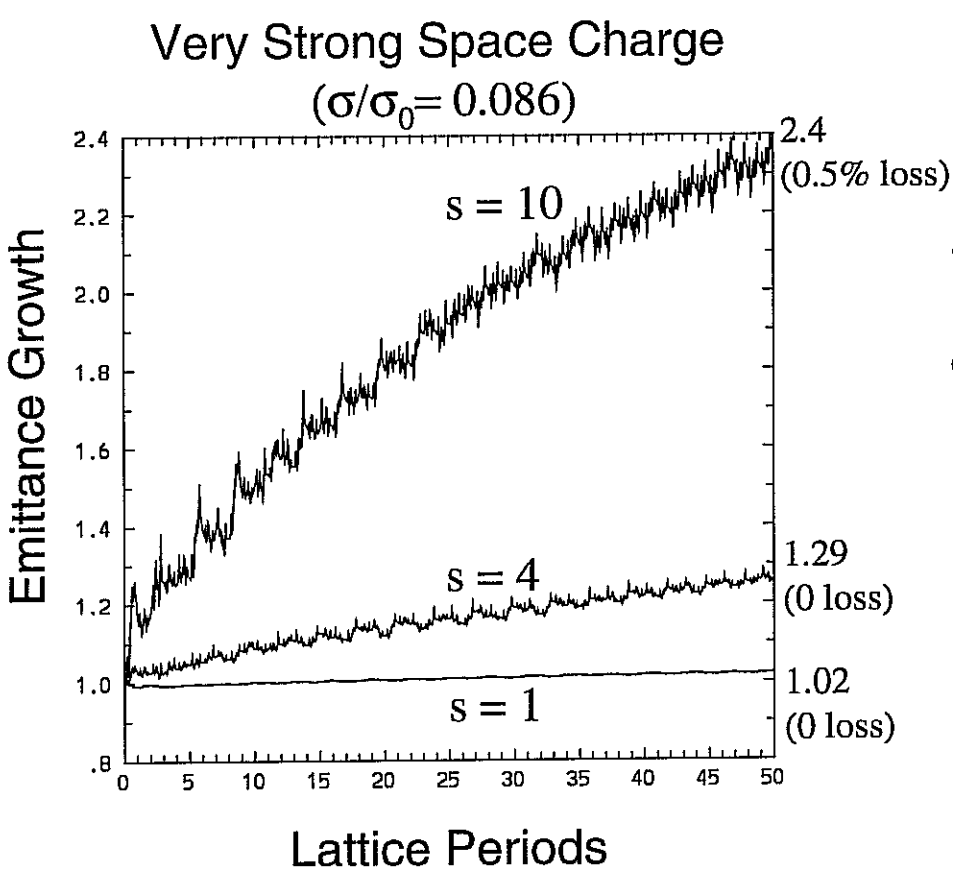

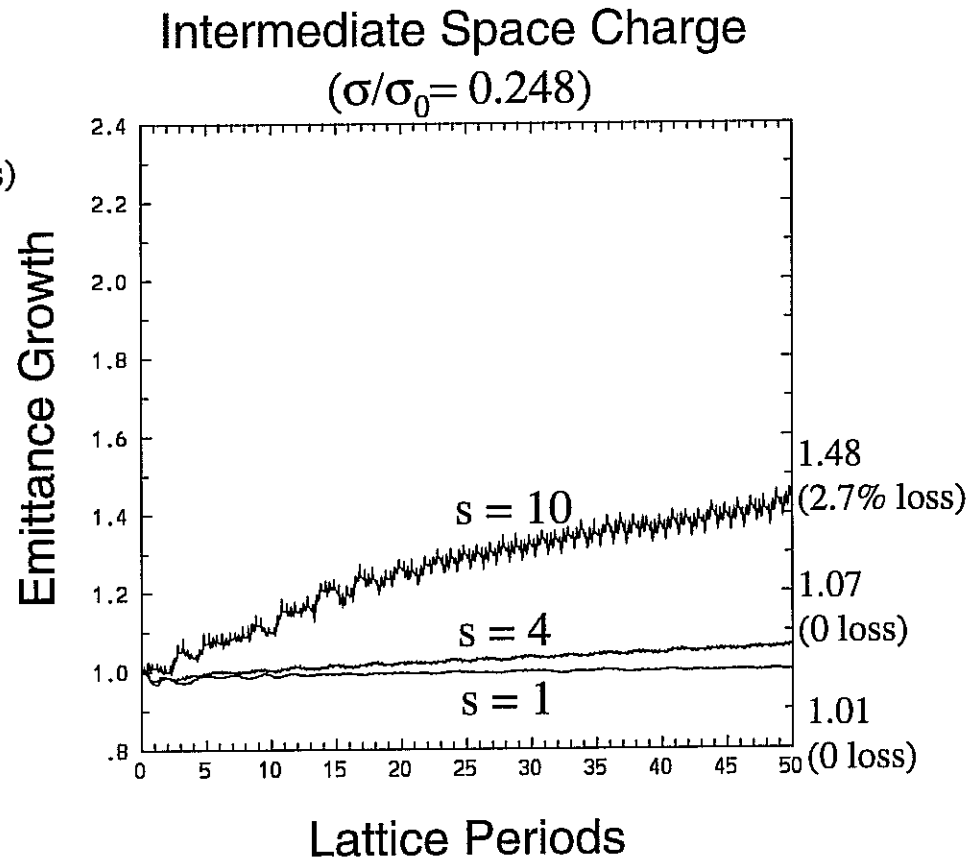

S.M. Lund 6/1

Initial KV Distribution

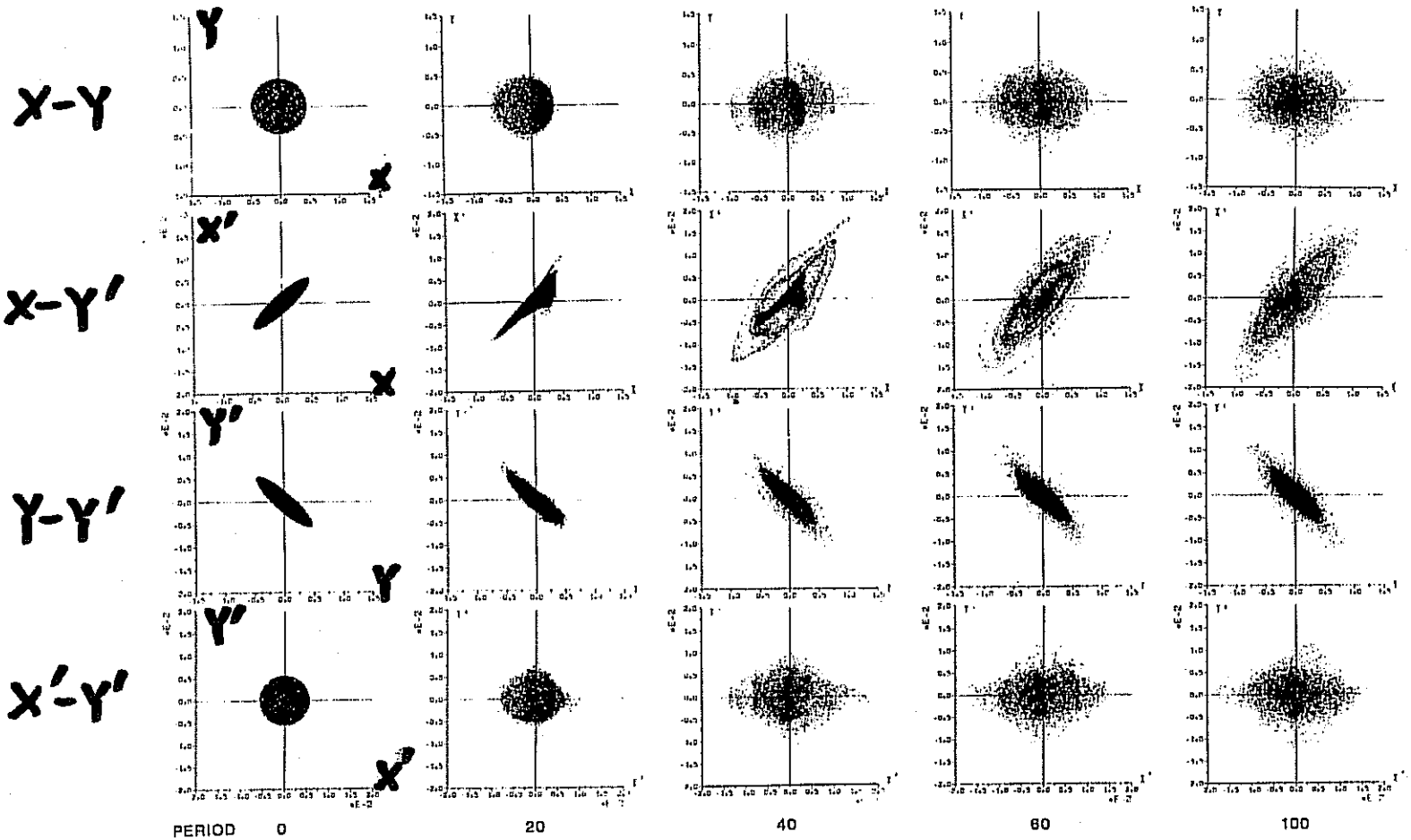

FIGURE 2 Transformation of an initial K-V distribution through the GSI FODO channel at $\sigma_0 = 90°$, $\sigma = 41°$.

J. Struckmeir, J. Klabunde, and M. Reiser, Part. Accel. 15, 47 (1984).

See also Reiser Text, pg 495.

S.M. Lund 6/

Initial Gaussian Distribution

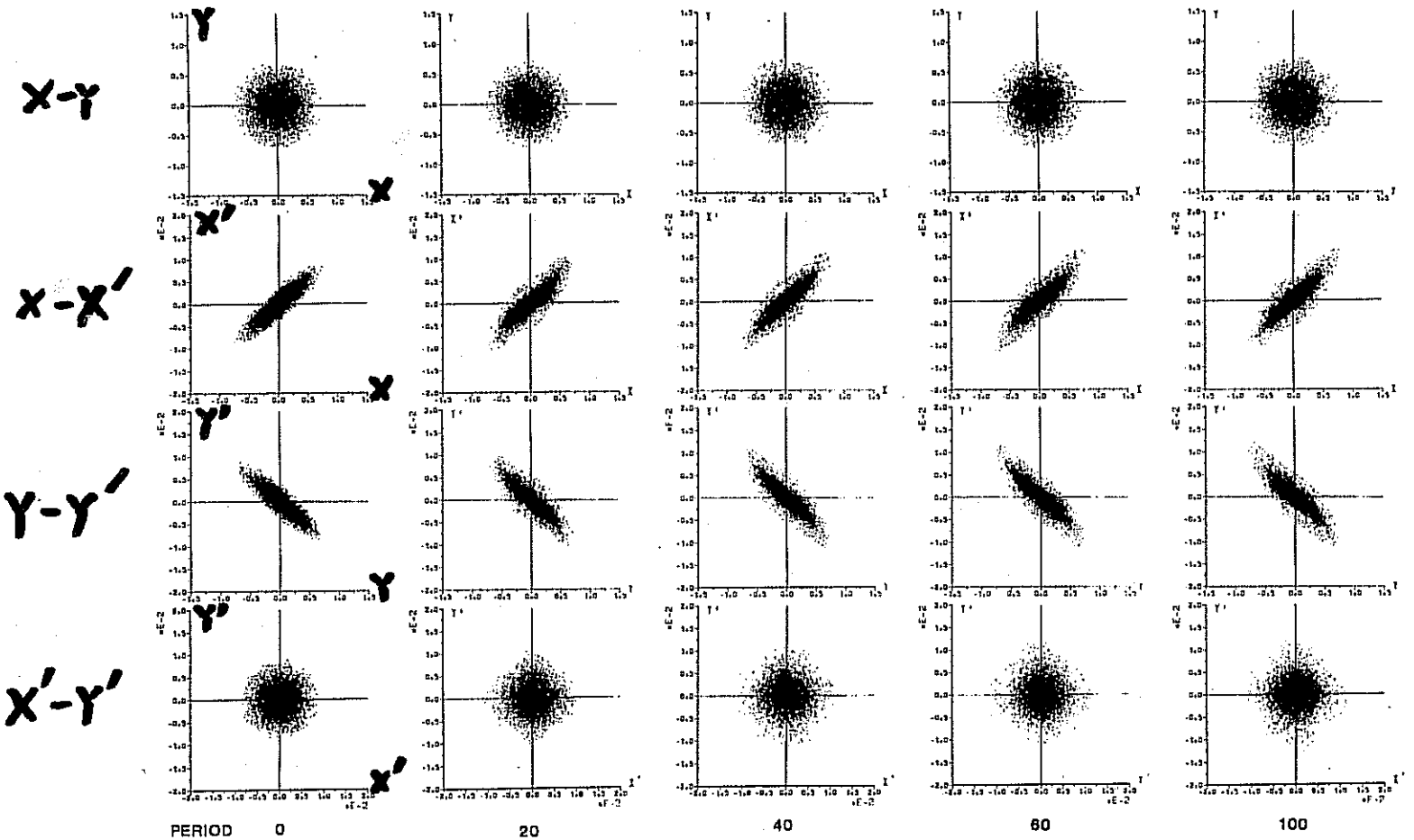

FIGURE 6 Transformation of an initial Gaussian distribution (rms-matched) through the GSI FODO channel at $\sigma_0 = 90°$, $\sigma = 41°$.

J. Struckmeier, J. Klabunde and M. Reiser, Part. Accel. 15, 47 (1984)

SM, Lund 63/

S. M. Lund 6/4/

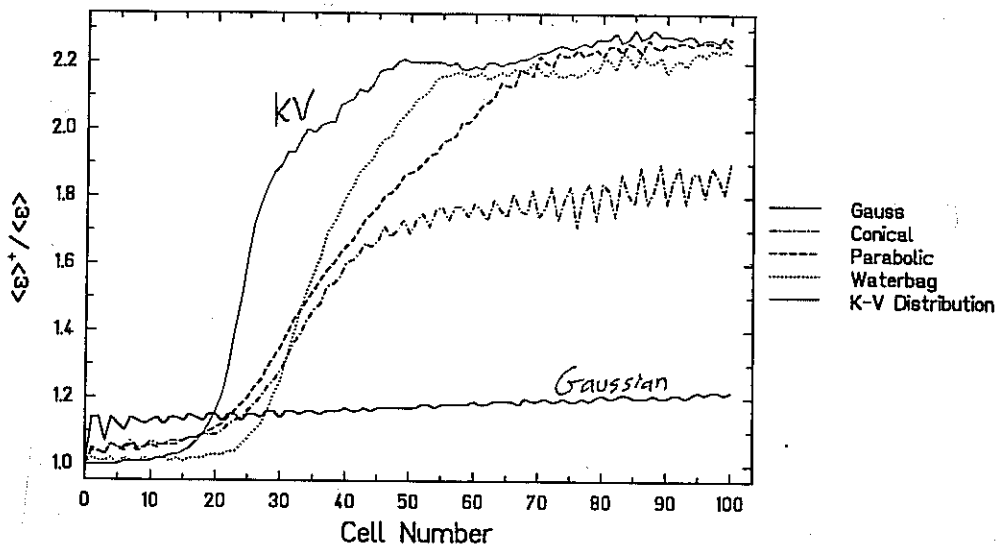

FIGURE 7 Emittance growth factors versus the number of cells obtained from particle simulations for initial K-V, waterbag, parabolic, conical and Gaussian distributions at $\sigma_0 = 90°$, $\sigma = 41°$.

From J. Struckmeier, J. Kabunde, and M. Reiser, Part. Accel. 15 47 (1984).

Distribution Methods – Direct Gridded Solution of Vlasov's Equation.

Consider the Vlasov equation as an example.

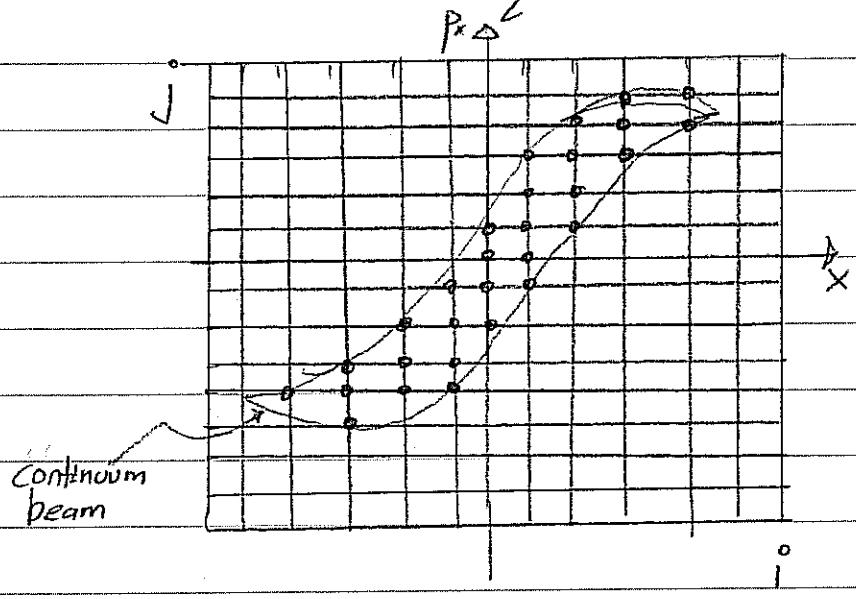

$$f(x_i, p_j, t) = f_{ij}(t)$$

The distribution is advanced at discrete grid points in time.

- Fields are typically solved using a discrete spatial mesh as for the particle methods described before.
  - Deposition on mesh is typically straightforward in Vlasov case (sum over momentum variable).

- The distribution advance cycle is different than for particle methods.
  - Numerical stability is key.
  - Characteristics and "semi-Lagrangian" methods can be employed.
  - Methods for solving for characteristics are familiar from dynamics/plasma physics.

Direct Vlasov Methods:

S. M. Lund 6/6/

"Pros"

Reasons for Vlasov simulations:

- Low noise - only discretization effects without statistical effects
- Allows clear analysis of collective effects and tenuous distribution components.

"Cons"

Reasons why Vlasov simulations are presently employed less than PIC:

- Extreme memory requirements for needed grid resolution in multi-dimensional phase space.
  - Beams often have sharp edges in phase space that move in responce to varying applied focusing forces.
- Numerical stability tends to be more difficult than in particle methods.

No time to illustrate Vlasov and other distribution methods in this introductory course. We hope to cover these methods and other numerical fieldsolve techniques in a later expanded version of this class.

However ..... it is easy to generalize from what we have learned!